Phase-field modeling of nanoscale island dynamics

Zhengzheng Hu[1], Shuwang Li[1], John Lowengrub[1], Steven Wise[2], Axel Voigt [3]

[1]Department of Mathematics, University of California, Irvine. CA 92697, United States
[2]Department of Mathematics, University of Tennessee, Knoxville, TN 37996, United States
[3]Caesar Research Center, Friedensplatz 16, 53111, Bonn, Germany.

Keywords: Epitaxial growth, Island dynamics, Morphological stability, Attachment-detachment, Desorption

Abstract

We present a phase-field model to simulate the dynamics of a perturbed circular island during epitaxial growth. Surface diffusion and a far-field flux are incorporated in the model. Moreover, a modified free energy function together with a correction to the initial phase variable profile is given to efficiently capture the morphological evolution when a large deposition flux is imposed. To test the algorithm, we present simulations involving both stable and unstable growth.

Introduction

Epitaxial growth is a means to produce almost defect-free, high quality single crystals that have a wide range of applications including advanced electronic and optoelectronic devices (e.g. see [6, 7]). During the early stages of epitaxial growth, adatoms on the surface often form small, circular shaped and widely separated islands [10, 11]. A comprehensive morphological stability analysis of this type of islands has been presented by Z. Hu et al. in [12]. They also suggested a way to control the shape of the island using the deposition flux and far-field flux as control parameters. In this paper, a phase-field model is presented and used to simulate the instabilities during the epitaxial growth. We propose a different free energy function than the one appeared in [17] by Rätz et al.. Advantages of using a phase-field approach include the automatic capture of topological changes such as island formation, coalescence and coarsening. In addition, other physical effects such as nucleation and elastic interactions may be included. Previously, finite element methods have been used to demonstrate the Ehrlich-Schwoebel and inverse Ehrlich-Schwoebel barrier during the island growth in [13, 14, 15]. But none of these methods considered combined effects of surface diffusion, Ehrlich-Schwoebel barrier and desorption.

The classical approach of Burton, Cabrera and Frank [5] (BCF) is to formulate a step-flow model in which the growth direction is discrete but the lateral direction is continuous. Let $\rho_\pm = \rho_\pm(x, y, t)$ be the adatom concentration on terraces $\Omega_\pm(t)$, where Ω_+ is one lattice width higher than Ω_-. Then, the BCF model is

$$\partial_t \rho_\pm - \nabla \cdot (D \nabla \rho_\pm) \;=\; F - \tau^{-1} \rho_\pm \quad \text{in } \Omega_\pm(\mathrm{t}), \tag{1}$$

where D is the diffusion constant, F is the deposition flux rate and τ^{-1} is the desorption rate. At the island edge $\Gamma(t) = R(\theta, t)$, the adatom concentration satisfies the kinetic boundary

conditions

$$-D\nabla\rho_+ \cdot \mathbf{n} = k_+ (\rho_+ - \rho^* (1 + \sigma\kappa)) \quad \text{on } \Gamma(\text{t}), \tag{2}$$

$$D\nabla\rho_- \cdot \mathbf{n} = k_- (\rho_- - \rho^* (1 + \sigma\kappa)) \quad \text{on } \Gamma(\text{t}), \tag{3}$$

where $\mathbf{n}$ is the unit normal pointing from the island to lower terrace, k_+ and k_- are the kinetic attachment rates from the island and lower terrace respectively, ρ^* is the equilibrium value of the adatom concentration for a straight step, σ is the line tension and κ is the curvature of $\Gamma(t)$. The normal velocity of the island edge is given by

$$V = -D\nabla\rho_+ \cdot \mathbf{n} + D\nabla\rho_- \cdot \mathbf{n} + \nabla_s \cdot (\nu\nabla_s\kappa) \quad \text{on } \Gamma(\text{t}), \tag{4}$$

where ν is the surface diffusion coefficient and $\nabla_s = (I - \mathbf{nn})\nabla$ is the surface gradient. See, [5, 8, 1, 9] for details. We also assume that the island and the lower terrace are enclosed in a large, fixed circle Γ_∞ with radius R_∞, and an additional far-field flux J is imposed along the outer circle

$$\frac{1}{2\pi}\int_{\Gamma_\infty} D\nabla\rho_- \cdot \mathbf{n}\, d\Gamma = J \quad \text{on } \Gamma_\infty, \tag{5}$$

where $\mathbf{n}$ is the unit exterior normal at Γ_∞. This flux could arise due to the diffusion of adtoms from other regions of the thin film and as such, it is a simple model of the effect of far-field interactions on the island nano-enviroment. (See [16] for a more realistic boundary condition which is based on a self-consistent mean-field theory.)
In this paper we will focus on the case in which the evolution is quasi-steady. That is, when the time scale for adatoms diffusion is much smaller than the time scale for deposition: $l_T^2/D << 1/F$ where l_T is a typical terrace width. Under this assumption, Eq. (1) reduces to

$$-\nabla \cdot (D\nabla\rho_\pm) = F - \tau^{-1}\rho_\pm \quad \text{in } \Omega_\pm(\text{t}), \tag{6}$$

while the other equations do not change.

Nondimensionalization

Time and space are non-dimensionalized by using the diffusion time scale $t^* = R_\infty^2/D$ (assume D is constant) and the length scale $l^* = R_\infty$ which is the radius of Γ_∞. And we introduce the modified adatom concentration $\omega_+ = \rho_+ - \rho^*$ (for the island) and $\omega_- = \rho_- - \rho^* - \Psi r$ (for the lower terrance), where r is the non-dimensional radial distance to the center of Ω_+. The resulting equations (given in [18]) depend on the following non-dimensional parameters

$$\Lambda = \frac{FR_\infty^2}{D}, \quad \mu = \frac{R_\infty}{\sqrt{D\tau}}, \quad \xi_\pm = \frac{D}{k_\pm R_\infty}, \quad \delta = \frac{\sigma}{R_\infty}, \quad \Psi = \frac{J}{D}, \quad \beta = \frac{\nu}{DR_\infty},$$

which are non-dimensional measures of the deposition flux rate, the desorption rate, the attachment rates, the line tension, the modified far-field flux and the surface diffusion, respectively.

Phase-field model

In the phase-field approach, the island boundary is treated as a diffuse interface with thickness ϵ^*, in order to match the non-dimensional model, we use $\epsilon = \epsilon^*/l^*$. Both island and

lower terrace can be viewed as separate phases of the system and accordingly is described by a phase-field variable ϕ^ϵ. The phase function ϕ^ϵ also can be interpreted as a continuous height function of the growing film. By extending the studies of the Rätz et al. [17], we present a modified phase-field model to account for surface diffusion and a far-field flux:

$$\begin{aligned} \partial_t\phi^\epsilon + \beta(\nabla_s\cdot\nabla_s k)|\nabla\phi^\epsilon| &= \nabla\cdot\left(M\left(\phi^\epsilon,\epsilon\right)\nabla(\omega^\epsilon+\Psi(1-\phi^\epsilon)r)\right)+\Lambda \\ &- \mu^2(\omega^\epsilon+\Psi(1-\phi^\epsilon)r+\rho^*), \qquad (7) \\ \alpha\epsilon^2(\partial_t\phi^\epsilon + \beta(\nabla_s\cdot\nabla_s k)|\nabla\phi^\epsilon|) &= \epsilon^2\Delta\phi^\epsilon - G'(\phi^\epsilon) + \frac{\epsilon}{\rho^*\delta}(\omega^\epsilon+\Psi(1-\phi^\epsilon)r)), \qquad (8) \end{aligned}$$

where ω^ϵ is the approximate adatom density, $\beta(\nabla_s\cdot\nabla_s k)|\nabla\phi^\epsilon|$ accounts for the effects of surface diffusion, $M(\phi,\epsilon)$ is the (anisotropic) mobility, $\Psi(1-\phi^\epsilon)r$ is used to account the far-field flux, α is a phase-field parameter, and $G(\phi)$ is the multi-well free energy function:

$$G(\phi) = w(e^{4.5\phi^2+0.9\phi^4}-1)(e^{4.5(1-\phi)^2+0.9(1-\phi)^4}-1), \quad \phi\in[0,1], \qquad (9)$$

where w is such that $\int_0^1\sqrt{2G(\phi)}\,d\phi = 1$. Note that $G(1) = G(0)$ and G has the symmetry $G(i+1/2+\phi) = G(i+1/2-\phi)$. This energy function is different from the one appeared in [17] and it helps to more accurately model adatom mobility on the terraces when the deposition flux is large. To account for the Erhlich-Schwoebel barrier, the mobility is asymmetric:

$$M(\phi,\epsilon) = \frac{1}{1+\epsilon^{-1}\zeta(\phi)} \qquad (10)$$

where $\zeta(\phi) = \gamma\phi^p G(\phi)$ when $\phi\in[0,1]$. Further, γ and p satisfy the following equations:

$$\int_0^1\frac{\zeta(\phi)}{\sqrt{2G(\phi)}}(1-\phi)\,d\phi = \xi_-, \quad \int_0^1\frac{\zeta(\phi)}{\sqrt{2G(\phi)}}\phi\,d\phi = \xi_+ \qquad (11)$$

An asymptotic analysis in [18], shows that if the parameter α is taken to be

$$\alpha = \frac{1}{\rho^*\delta}\int_0^1\frac{\zeta(\phi)}{\sqrt{2G(\phi)}}(1-\phi)\phi\,d\phi, \qquad (12)$$

then phase-field model described above reduces to the quasi-steady BCF model with desorption, surface diffusion and far-field flux, at leading order in an asymptotic expansion in ϵ.

Numerical method

We solve the system (7)-(8) using nonlinear multigrid methods originally developed for Cahn-Hilliard equations by Kim, Kang and Lowengrub [2, 3]. These algorithms are based on splitting the fourth order Cahn-Hilliard equation into two second order equations and solving for the concentration and the phase-field variable simultaneously using second order accurate discretizations in time and space. The spatial discretizations use centered differences and are conservative. The time discretizations are based on generalizations of the Crank-Nicholson algorithm and are fully implicit, thus eliminating the high (fourth) order time step restrictions (i.e. $\Delta t \le C\Delta x^4$). In certain cases, it is possible to rigorously prove that the resulting numerical schemes converge [3] and that the schemes inherit a discrete version of the continuous energy functional for any time and space step sizes [2, 3].

To solve the nonlinear discrete system, a nonlinear full approximation storage (FAS) method is used. The convergence of our multigrid algorithms is achieved with $\Delta t \leq \Delta t_0$ where Δt_0 depends only on the physical parameters and not on the mesh size. Typically we find that our algorithms are 1000 times faster than corresponding explicit methods. In addition, block-structured Cartesian mesh refinement as described in [4] is used to provide extra efficiency.

Results

Our goal is to characterize the non-linear evolution of nanoscale islands to determine the extent of applicability of the linear stability theory and ideas on shape control as described in [12, 19]. In this paper, we present a preliminary result, in which the desorption rate, surface diffusion and far-field flux are absent, and the deposition flux is constant in time.

To simulate the growth of a circular island enclosed in a fixed circle, we use $[-1, 1]^2$ as the computational domain and scale the deposition flux by a cutoff function, specifically, a hyperbolic tangent function supported on the smeared unit disk. To demonstrate the instability, the deposition should be sufficiently large (see [12] for details). However, we found that the original phase-field model for island dynamics in [17] requires very small interface thickness to accurately capture the morphological evolution of the interface. This means, even though asymptotic analysis indicates the convergence in ϵ, the regime of applicability requires ϵ to be very small. To make the calculations possible and extend the applicability of the phase-field model, we introduce two modifications to the original model. The first is the modified new energy function shown in Eq. (9). The second is that the hyperbolic tangent initial profile of the phase variable is corrected by adding the first order outer solution of the phase variable from the asymptotic analysis. In fact, the correction term we add is $\epsilon\phi_1$, where $\phi_1 = \dfrac{\omega_{linear}}{\rho^* \delta G''(\phi_0)}$, ω_{linear} is the linear solution, and ϕ_0 is the hyperbolic tangent profile.

In Fig. 1[a], the evolution of a perturbed 5-fold island under a constant flux is shown. The island boundary is defined by $R(\theta, 0) = R(0)(1 + P(0)cos(5\theta))$ with radius $R(0) = 0.228$ and shape factor $P(0) = 0.087$, initially. We used $\epsilon = 0.00625$, and 7 levels of mesh refinements with 16 grid points on the coarsest mesh and 2048 grid points at the finest level in each coordinate direction. There are approximately 6 computational nodes across the island interface. The time step $\Delta t = 2 \times 10^{-7}$ and the islands are shown at non-dimensional times $t = 0$, $t = 0.0030$, $t = 0.0066$, $t = 0.0102$, $t = 0.0138$, and $t = 0.0174$. As seen from the figure, the island undergoes unstable growth initially but the perturbations start to decrease as the island becomes large enough. This result matches our linear stability analysis result presented in [12]. The information regarding the mesh refinement is given at two different times: $t = 0$ and $t = 0.0174$ in [b] and [c]. Slices of the concentration ω^ϵ at $y = 0$ are shown in [d]. We observe from the zoom-in plot that the concentration has a near jump at the island boundary, which is consistent with the classical theory. Moreover, the radii of the underlying circle $R(t)$ during the evolution are plotted versus time in [e], in which the linear theory is given in the solid line and the numerical result is given in the dash-dot line. Clearly, the numerical result matches the linear theory very well. In [f], the evolution of the shape factors $P(t)$ is shown. Again, the solid line is the linear prediction and the dash-dot line is the numerical result. We observe that the linear theory over-predicts the growth the of perturbation.

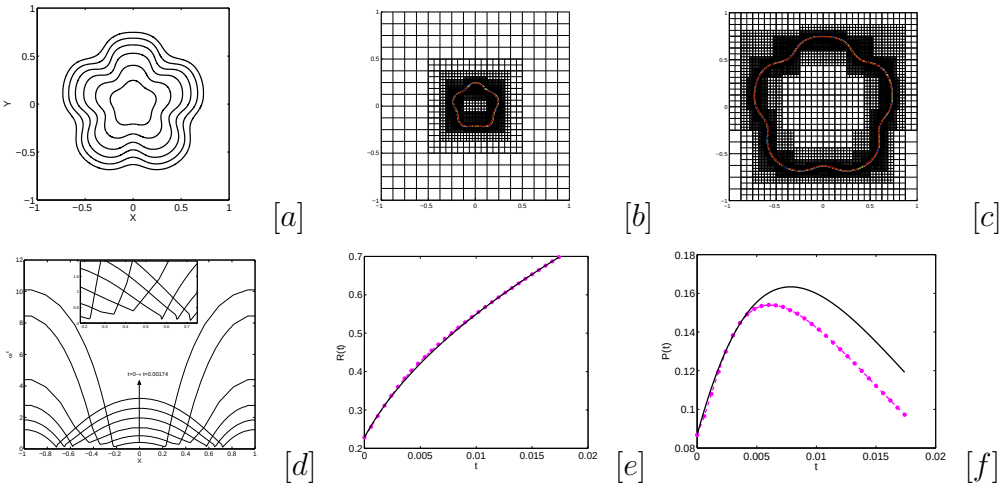

Figure 1: $[a]$. The evolution a 5-fold island under a constant deposition flux at 6 times: $t = 0$, $t = 0.0030$, $t = 0.0066$, $t = 0.0102$, $t = 0.0138$, and $t = 0.0174$. $[b]$ and $[c]$. The mesh snap-shots at the initial time and the final time. $[d]$. Slices of the concentration at $y = 0$ corresponding to the times shown in $[a]$. $[e]$. The radii of the underlying circle during the evolution versus the time. The solid curve is the solution of the linear analysis and the dash-dot line is the numerical solution. $[f]$. The evolution of the shape factors versus time. The non-dimensional parameters are: $\lambda = 25$, $\xi_+ = 0.0256$, $\xi_- = 0.002$, $\rho^* = 1$, $\delta = 0.02$, $\beta = 0.0$, $p = 20$.

Conclusions and future work

An efficient, second order accurate finite difference scheme and adaptive mesh refinement method were used to simulate a phase-field model of the dynamics of islands during the epitaxial growth. A new phase-field that accounted the effects of surface diffusion and a far-field flux was presented. Moreover, two modifications were given to extend the applicability of the phase-field model to more accurately simulate the island morphologies. Our numerics showed that the growth of the underlying circle matches the linear theory very well, whereas the linear theory over-predicts the growth of the perturbations. We are currently investigating the morphology changes when a variable (in time) flux is used to control the shape of the island at the nanoscale. In future work, we will investigate the effects of the surface diffusion and elastic interactions as these phenomena can play a critical role in island dynamics.

Acknowlegements

The authors gratefully acknowledge partial support from the National Science Foundation Division of Mathematical Sciences and the Division of Materials Research. Z. Hu was also partially supported by a Doctoral Dissertation Fellowship from the Graduate School at the University of California, Irvine. The authors also acknowledge the generous computing resources from the Network and Academic Computing Services.

References

[1] J. Krug. "Introduction to step dynamics and step instabilities", in A. Voigt. editor, Multiscale Modeling in epitaxial growth, pages 79, Birkhauser, 2005.

[2] J. S. Kim, K. Kang, and J. S. Lowengrub. "Conservative methods for cahn-hilliard fluids", J. Comp. Phys., 193, 2003.

[3] J. S. Kim, K. Kang, and J. S. Lowengrub. "Conservative multigrid methods for ternary cahn-hilliard systems", Comm. Math. Sci., 2, 2004.

[4] S. Wise, J. Kim, J. Lowengrub. "Solving the regularized, strongly anisotropic Cahn-Hilliard equation by an adaptive nonlinear multigrid method", J. Comp. Phys., **226**, 1, 414, 2007.

[5] W. Burton, N. Cabrera, F. Frank, "The growth of crystals and the equilibrium structure of their surfaces", Phil. Trans. Roy. Soc. London, Ser. A **243**, 299, 1951.

[6] X. L. Wang, V. Voliotis, "Epitaxial growth and optical properties of semiconductor quantum wires", J. Appl. Phys., **99**, 121301, 2006.

[7] H. E. Katz, "Recent advances in semiconductor performance and printing processes for organic transistor-based electronics", Chem. Mater., **16**, 4748, 2004.

[8] R. E. Caflisch, B. Li, "Analysis of island dynamics in epitaxial growth of thin films", Multiscale Model. Simul., **1**, 150, 2003.

[9] R. Ghez, S. S. Iyer, "The kinetics of fast steps on crystal surfaces and its application to the molecular beam epitaxy of silicon", IBM J. Res. Develop., **32**, 804, 1998.

[10] K. Morgenstern, G. Rosenfeld, G. Comsa, "Decay of two-dimensional Ag islands on Ag(111)", Phys. Rev. Lett., **76**, 2113, 1996.

[11] W. Theis, N. C. Bartelt, R. M. Tromp, "Chemical potential maps and spatial correlations in 2D-island ripening on Si(001)", Phys. Rev. Lett., **75**, 3328, 1995.

[12] Z. Hu, S. Li, J. Lowengrub, "Morphological stability analysis of the epitaxial growth of a circular island: Application to nanoscale shape control", Physica D, **233**, 2, 151, 2007.

[13] F. Haußer, A. Voigt, "Finite element method for epitaxial island growth", J. Crystal Growth, **266**, 381, 2004.

[14] E. Bänsch, O. Lskkis, B. Li, F. Haußer, A. Voigt, "Finite element method for epitaxial growth with attachment-detachment kinetics", J. Comp. Phys., **194**, 409, 2004.

[15] E. Bänsch, F. Haußer, A. Voigt, Technical Report 36, Research Center Caesar, 2003.

[16] G. S. Bales and D. C. Chrzan, "Transition from compact to fractal islands during submonolayer epitaxial growth", Phy. Rev. Lett., **74**, 4879, 1995

[17] A. Rätz, A. Voigt, "Phase-field models for island dynamics in epitaxial growth", J. Crystal Growth, **266**, 278, 2004.

[18] Z. Hu, S. Li, J. Lowengrub, "Nonlinear simulations of nanoscale island dynamics", in preparation.

[19] S. Li, P. H. Leo, V. Cristini, "Nonlinear stability analysis of self-similar crystal growth: Control of the Mullins-Sekerka instability", J. Crystal Growth, **277**, 578, 2005.